K-6-01 (Invited)
Extended Abstracts of the 2019 International Conference on Solid State Devices and Materials, Nagoya, 2019, pp477-478

Carrier Scattering Mechanism in SiC Trench MOSFETs

Katsuhiro Kutsuki[1], Eiji Kagoshima[2], Toru Onishi[2], Jun Saito[2], Kensaku Yamamoto[3], Yukihiko Watanabe[1]

[1] TOYOTA CENTRAL R&D LABS., INC.
41-1, Yokomichi, Nagakute, Aichi 480-1192, Japan
Phone: +81-561-71-7498 E-mail: kutsuki-k@mosk.tytlabs.co.jp
[2] TOYOTA MOTOR CORPORATION
543, Kirigahora, Nishihirose-cho, Toyota, Aichi 470-0309, Japan
[3] DENSO CORPORATION
500-1, Minamiyama, Komenoki-cho, Nisshin, Aichi 470-0111, Japan

Abstract

To reduce the channel resistance of 4H-SiC trench MOSFETs, improvement of the channel mobility is necessary. The experimental evaluation technique of channel mobility and carrier scattering mechanism have been investigated. It was found that Coulomb scattering and optical phonon scattering were the limiting factors of channel mobility in the low- and high-temperature regions, respectively.

1. Introduction

From the viewpoint of reduction of channel resistance (R_{ch}), one of the most promising device structures is the trench-type MOSFETs (UMOSFETs) which could enlarge the channel width by reduction of cell pitch [1]. Although studies have demonstrated several types of trench MOSFETs with relatively small specific on-resistance [2-6], the channel mobility is lower than that for lateral type MOSFETs. Reported field effect channel mobility (μ_{eff}) are in the range of only 5-50 cm^{2}V^{-1}s^{-1}. To improve channel mobility in SiC trench MOSFETs, a comprehensive understanding of the carrier scattering mechanism is necessary.

In this study, a method for evaluating the channel mobility by eliminating parasitic series resistance in trench MOSFETs as shown in Fig. 1 is proposed, then the carrier scattering mechanism is investigated.

2. Experimental methods

The isolated one-cell trenched MOSFET with n-channel was fabricated on 4H-SiC epitaxial layer grown on heavily doped n$^+$-type SiC (0001) substrate as shown in Fig. 1. The acceptor concentration (N_A) was 1 × 10^{17} cm^{-3}. After the source and drain region had been formed, the trench gate was fabricated. Nitridation was performed following deposition of a 75-nm-thick gate oxide in order to reduce the interface state. To analyze components of mobility, the drain current-gate voltage (I_D-V_G) characteristics of fabricated MOSFETs were measured at the temperature in the range from 233 to 523 K. The body layer was fixed at ground potential, and the drain voltage (V_D) was 0.1 V.The measurement using the drain electrode on the back surface ("DOWN" in Fig. 1) and that using the drain electrode on the surface ("UP" in Fig. 1) were performed.

3. Results and discussion

3.1 Separation of R_{ch} from series resistance

Figures 2 show the temperature dependence of normalized I_D-V_G characteristics for DOWN and UP measurements. In the case of UP measurements, the impact of temperature was drastically reduced compared to that of DOWN measurements. Since the largest component of series resistance in Fig. 1 is the resistance of drift layer (R_D), the temperature dependence by DOWN measurement is considered to be mainly caused by R_D. Figure 3 shows the values of R_{ch} and R_D obtained at each measurement temperature. The UP measurements provide R_{ch} and the DOWN measurements provide the sum of R_{ch} and R_D. The result reveals a strong temperature dependence of R_D, which suggests that separating R_D from R_{ch} is extremely important in the analysis of the inversion carrier effective mobility [7,8]. This strong temperature dependence of R_D can result from the optical phonon scattering of the bulk SiC in the drift layer [9].

3.2 Carrier scattering mechanism

Figure 4 shows the temperature dependence of μ_{eff} calculated from I_D-V_G characteristics as shown in Fig. 2(b) [10,11]. μ_{eff} was further analyzed based on a mobility model that includes μ_{OP} [12,13]. Optical phonon scattering, which is taken into account in the bulk mobility of GaAs [14], GaN [15], and SiC [9], has been reported to have a large impact on total mobility (Fig. 5). Therefore, instead of acoustic phonon scattering mobility, which is used in conventional mobility models [16,17], μ_{OP} is adopted in the improved mobility model along with Coulomb scattering mobility (μ_C) and surface roughness scattering mobility (μ_{SR}). Figure 6 shows the temperature dependence of each mobility component (μ_C, μ_{OP}, and μ_{SR}) obtained at E_{eff} = 1 MVcm^{-1}. In the low temperature region (≤ 298 K), μ_C was found to be the limiting factor of μ_{total}. In the high temperature region (≥ 423 K), μ_{total} was limited by μ_{OP}, which depends on the material properties.

4. Conclusions

To separate R_{ch} experimentally, the UP measurement method was proposed. From the temperature dependence of mobility factors obtained using UP measurements, it was found that μ_C and μ_{OP} were the limiting factors of μ_{eff} in the low- and high-temperature regions, respectively.

References

[1] T. Kimoto, Jpn. J. Appl. Phys. **54**, 040103 (2015).
[2] C. T. Banzhaf *et al.*,Material Science Forum **821-823**, 753 (2015).
[3] Y. Kagawa *et al.*, Mater. Sci. Forum **821-823**, 761 (2015).
[4] S. Harada *et al.*, IEEE Electron Device Lett. **37**, 314 (2016).
[5] D. Peters *et al.*, Proceedings of the 29th ISPSD, p239.
[6] T. Masuda *et al.*, IEDM2018 Tech. Dig. p.177.
[7] M. Hauck *et al.*, Communications Physics **2**, 5 (2019).
[8] K. Kutsuki *et al.*, Solid State Electronics, *in press*.
[9] J. Pernot *et al.*, J. Appl. Phys. **90**, 1869 (2001).
[10] K. Kutsuki *et al.*,, Mater. Sci. Forum **821–823**, 757 (2015).
[11] K. Kutsuki *et al.*,, Mater. Sci. Forum **858**, 607 (2016).
[12] K. Kutsuki *et al.*, JJAP **56**, 04CR03 (2017).
[13] K. Kutsuki *et al.*, JJAP **57**, 04FR02 (2018).
[14] C. M. Wolfe *et al.*, J. Appl. Phys. **41**, 3088 (1970).
[15] D. Zanato *et al.*, Semicond. Sci. Technol. 19, 427 (2004).
[16] S. Takagi *et al.*, IEEE Trans. Electron Devices **41**, 2357 (1994).
[17] M. Noguchi *et al.*, IEDM2017 Tech. Dig. p.219.

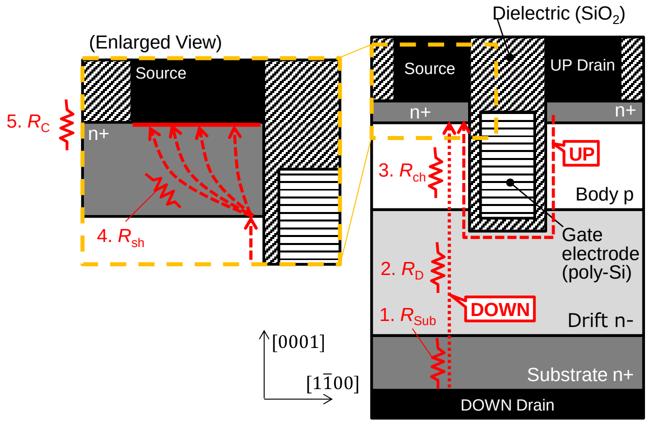

Fig. 1 Cross-sectional image of isolated one-cell trench MOSFETs. Current paths and resistance components are also shown.

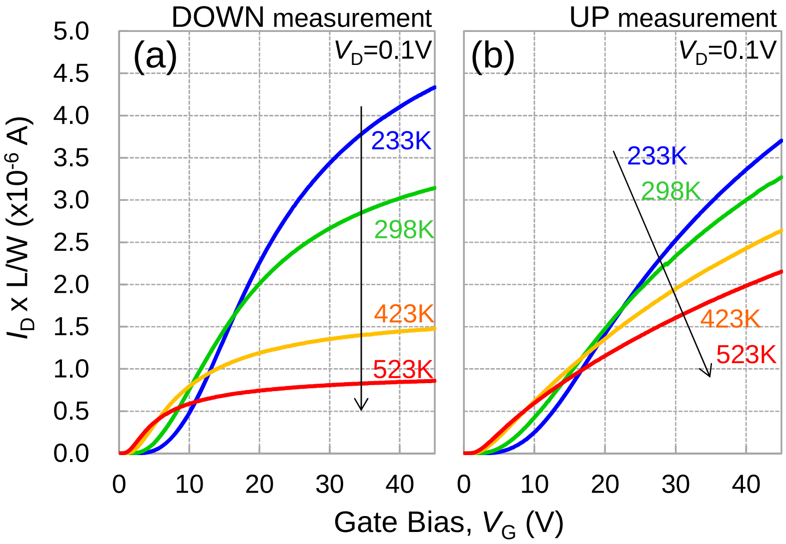

Fig. 2 Temperature dependence of I_D-V_G characteristics normalized by the channel length (L) and the channel width (W). Results of (a) DOWN and (b) UP measurements were shown.

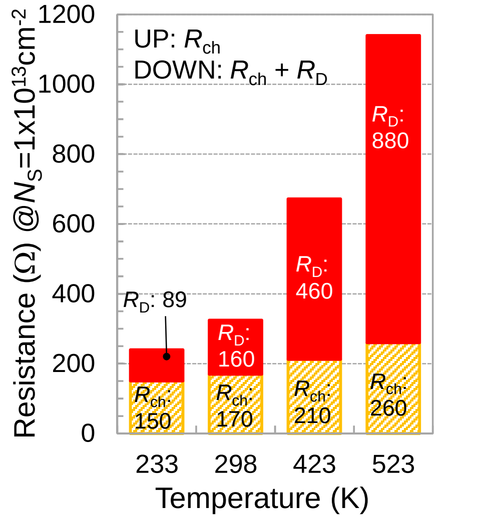

Fig. 3 Values of R_{ch} and R_D obtained at each temperature. UP measurements give R_{ch}, and DOWN measurements give the sum of R_{ch} and R_D.

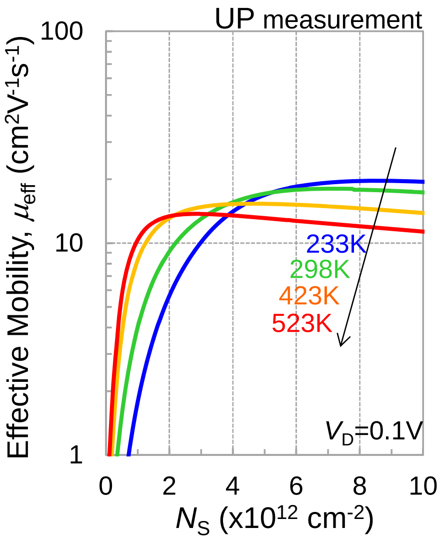

Fig. 4 Temperature dependence of effective mobility obtained from UP measurements.

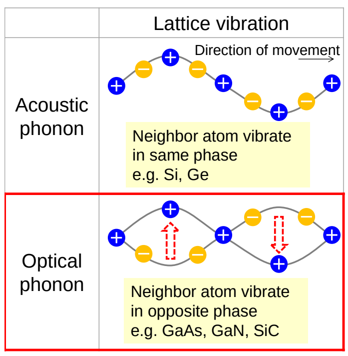

Fig. 5 Images of lattice vibration in crystal. An acoustic phonon vibrates in the same phase as the next phonon (e.g. Si, Ge), while an optical phonon vibrates in the opposite phase (e.g. GaAs, GaN, SiC).

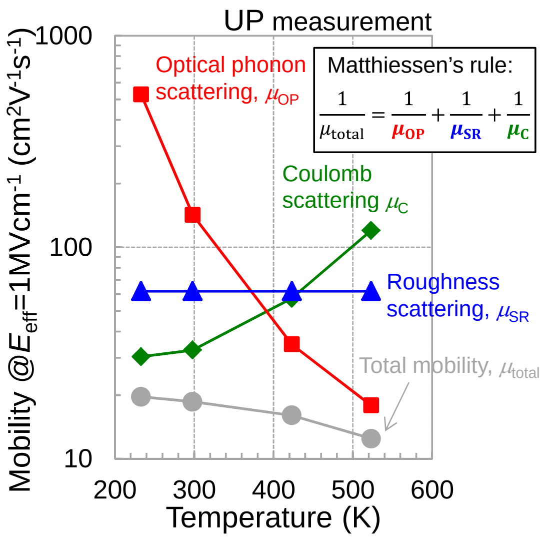

Fig. 6 Temperature dependence of mobility factors obtained at E_{eff} = 1 MVcm^{-1} from UP measurements.